

Low-temperature heat capacity and magnetic properties of the $RNiX_2$ compounds ($R = \text{La, Ce}$; $X = \text{Si, Ge, Sn}$)

V. K. Pecharsky* and K. A. Gschneidner, Jr.

Ames Laboratory and Department of Materials Science and Engineering, Iowa State University, Ames, Iowa 50011

L. L. Miller

Ames Laboratory, Iowa State University, Ames, Iowa 50011

(Received 19 July 1990; revised manuscript received 17 December 1990)

Heat-capacity (1.4–80 K) and magnetic-susceptibility (1.5–300 K) measurements were carried out for the series of six ternary intermetallic compounds with $RNiX_2$ composition ($R = \text{La, Ce}$ and $X = \text{Si, Ge, and Sn}$). All of the $LaNiX_2$ compounds exhibit normal metallic behavior with an electronic specific-heat coefficient in the range 5.2–5.6 mJ/mol K² and Debye temperature decreasing from 451 K ($LaNiSi_2$) to 258 K ($LaNiSn_2$). The $CeNiX_2$ compounds display anomalous behaviors. $CeNiSi_2$ is an intermediate-valence compound at high temperatures with the cerium valence varying from 3.35+ at room temperature to 3.65+ at $T = 50$ K, and becomes a spin fluctuator at low (around 3.3 K) temperature. The spin fluctuations can be quenched by an external magnetic field of about 5.3 T. Both $CeNiGe_2$ and $CeNiSn_2$ undergo two-step antiferromagnetic phase transitions at $T_N^I = 3.9$ K and $T_N^II = 3.2$ K, which are accompanied by sharp anomalies for all properties studied. The electronic specific constants (in units of mJ/mol Ce K²) of the three Ce compounds were 45.3 ± 0.6 for $CeNiSi_2$, 97.6 ± 0.9 for $CeNiGe_2$, and 60.8 ± 0.7 for $CeNiSn_2$.

INTRODUCTION

Ternary rare-earth intermetallic compounds are the subject of continuous interest for experimental studies of their physical behaviors because, simultaneously with simple, easily interpreted properties, they sometimes exhibit complicated or even unique ones. Of the vast number of rare-earth ternary compounds, the majority of the different compositions and crystal structures vary in a systematic and logically understood fashion: however, the occurrence of unusual or anomalous behaviors is often caused by small compositional or crystal structural changes, especially when cerium is the rare-earth component. Intermetallides containing silicon, germanium, or tin as one of the components are of special interest, because these elements represent the series with transition from semiconducting (Si) to typically metallic (Sn) features, and in many cases the crystal structures of appropriate ternary compounds remain the same or at least closely related to each other.

This paper is a report on the investigation of the low-temperature magnetic behaviors and heat capacity of a series of intermetallic compounds with composition $RNiX_2$, where $R = \text{La or Ce}$, and $X = \text{Si, Ge, or Sn}$. Crystallographic studies by Bodak and Gladyshevsky¹ ($X = \text{Si, Ge}$) and Skolozdra and Komarovskaya² ($X = \text{Sn}$) indicated that all of the compounds crystallized in the $CeNiSi_2$ type structure. Four of these six compounds, namely, those containing silicon and germanium, are characterized by a completely ordered atomic distribution in the lattices.¹ According to Skolozdra and Komarovskaya,² the $RNiSn_2$ compounds ($R = \text{La, Ce}$) are also completely ordered at ideal stoichiometry, but, in addition, form

solid solution alloys which have a deficiency of nickel atoms, and thus the composition formula can be written as $RNi_{1-x}Sn_2$, where $0 < x < 0.49$.²

Only the high-temperature (78–300 K) magnetic susceptibility has been reported for $CeNiSi_2$ (Ref. 3) and $CeNiSn_2$.² It was found that both compounds are paramagnetic, and their susceptibilities obey the Curie-Weiss law. The effective magnetic moments and paramagnetic Curie temperatures derived from the χ^{-1} versus T dependences were found to be as follows: $\mu_{\text{eff}} = 2.60\mu_B$, $\theta_p = -150$ K (this temperature in the absolute sense is surprisingly high), and $\mu_{\text{eff}} = 2.43\mu_B$, $\theta_p = 5$ K for $CeNiSi_2$ and $CeNiSn_2$, respectively.

EXPERIMENTAL DETAILS

The lanthanum and cerium used in this study were prepared at the Materials Preparation Center of the Ames Laboratory, while the other metals were purchased from commercial sources. The lanthanum was 99.79 at. % pure, with main impurities H-0.17, N-0.01, and O-0.02 at. %; the cerium was 99.93 at. % pure, with main impurities C-0.015 and O-0.04 at. %; the silicon, germanium, and tin were 99.999 wt. % pure; and the nickel was 99.5 at. % pure, with main impurities H-0.29, C-0.24, and O-0.01 at. %.

All ternary compounds with a nominal composition $RNiX_2$ were prepared by arc-melting pieces of metals in an argon atmosphere on a water-cooled copper hearth and then annealed at 1000°C in helium-filled sealed quartz tubes for 50 h. During arc melting, weight losses were less than 0.4% of total mass, which was about 5 g for each sample. Phase and crystal structure analyses

were performed by means of metallography and x-ray powder diffractometry. Metallographic analyses indicated that the samples used in this study were essentially single phase. Room-temperature x-ray-diffraction patterns were measured by using Cu $K\alpha$ graphite monochromated radiation, microcomputer-controlled SCINTAG powder diffractometer. In addition to determining the lattice parameters a comparison of the observed intensities with the calculated ones indicated that the compounds were completely ordered, with the respective atoms occupying the correct sites of the CeNiSi₂ structure. Low-temperature zero-field (1.4–80 K) and magnetic-field (1.4–20 K) heat capacities were measured using adiabatic heat pulse type calorimeter.⁴ Magnetic susceptibility from 1.6 K up to room temperature was measured in a field of 0.66 T by using a Faraday microbalance.⁵ Low-field magnetization (2–25 K) data were taken using a SQUID magnetometer. All measurements were controlled by microcomputers.

RESULTS AND DISCUSSION

Crystal structures

All of the synthesized compounds were found to be single phase and to have the CeNiSi₂-type structure. The refined lattice parameters (using a least-square procedure⁶) are listed in Table I together with the reported values. As one can see, they are in satisfactory agreement except for LaNiSn₂ and CeNiSn₂, where there is a significant difference in the *b* lattice parameters. It is difficult to explain such a remarkable difference for just one (the largest) of the three independent unit-cell dimensions in both cases. Our results seem to be at least more reasonable, because when all three of the unit-cell dimensions for CeNiSn₂ are compared with those of LaNiSn₂, the cerium values are consistent with lanthanide contraction on going from lanthanum to cerium. Previously reported results by Skolozdra and Komarovskaya² (SK) show an increase in the *b*-cell dimension on going from LaNiSn₂ to CeNiSn₂. We believe that the lattice param-

eters reported by SK were determined on samples with nonstoichiometric compositions RNi_{1-x}Sn₂, where *x* for the lanthanum compound was greater than the *x* value for the cerium phase. We did not refine atomic parameters, since this has been done many times for different classes of compounds with the CeNiSi₂-type crystal structure and the results always gave similar values.

We would like to point out one important observation here. When one plots the unit-cell volume versus atomic number of the lanthanide elements for the same RNiX₂ compound series a slight minimum is found at CeNiSi₂ in the RNiSi₂ series, but none are found for CeNiGe₂ and CeNiSn₂ in their respective series of RNiX₂ phases. The appearance of such a minimum for Ce-containing (as well as maxima for Eu- and Yb-containing) compounds suggests the possibility of interconfiguration (or valence) fluctuation state between Ce³⁺ and Ce⁴⁺ (or Eu²⁺, Yb²⁺ and Eu³⁺, Yb³⁺).

Heat capacities

The experimental results of the zero-field heat-capacity measurements are shown in Figs. 1–3. Only the data below 20 K are presented, because at higher temperatures the heat capacities in all cases behave normally with increasing temperature up to 80 K. Below ~10 K all of the Ce-containing compounds exhibit anomalous features, while the lanthanum-containing compounds behave, as expected, as typical metallic compounds. It is especially important to note that the heat capacities of the CeNiX₂ compounds are parallel to those of the respective LaNiX₂ compound from at least 14 K up to 80 K. This indicates that the crystal-field splitting in the cerium compounds must be >100 K; otherwise, the parallelism would be destroyed by the occurrence of the Schottky anomaly, which begins to make itself manifest in the heat capacity at a temperature approximately one-half of the splitting energy in degrees Kelvin.

Before we report on information deduced from these measurements, we will briefly describe the procedure for

TABLE I. Lattice parameters of RNiX₂ compounds.

Compound	Lattice parameters (Å)			Reference
	<i>a</i>	<i>b</i>	<i>c</i>	
LaNiSi ₂	4.193	16.581	4.073	1
	4.2240(6) ^a	16.613(2) ^a	4.1022(5) ^a	This work
CeNiSi ₂	4.141	16.418	4.068	1
	4.1430(3)	16.406(1)	4.0636(3)	This work
LaNiGe ₂	4.3077(5)	16.904(1)	4.2373(5)	This work
CeNiGe ₂	4.244	16.747	4.199	1
	4.2536(4)	16.787(1)	4.2090(3)	This work
LaNiSn ₂	4.513	17.71	4.513	2
	4.509(1)	18.182(3)	4.524(2)	This work
CeNiSn ₂	4.485	17.74	4.485	2
	4.483(2)	17.934(5)	4.493(2)	This work

^aA least-squares estimated standard deviation in the least significant digit is given in parentheses.

determining the electronic specific-heat coefficient (γ) of the cerium compounds.

It is obvious that any attempt to directly fit the experimental data to the equation

$$C = \gamma T + \beta T^3 \quad (1)$$

will fail because of the presence of the anomalies in the CeNiX_2 phases. The best way to determine γ is to compare heat capacities of cerium compounds with the appropriate lanthanum ones at temperatures above the temperature of the anomalies in the cerium compounds. This is quite reasonable, since (i) lanthanum and cerium are the neighbors in the periodic system differing only by one $4f$ electron and have the same outer electron configuration ($6s5d$)³, since, as noted above, there is no anomaly in the unit cell volume versus atomic numbers plot at cerium; (ii) the assumption is that the lattice contributions (the βT^3 term in the above equation) to the heat capacity are the same because they have the same

crystal structure, similar lattice parameters (see Table I), and nearly the same mass. Therefore, the difference

$$\begin{aligned} \Delta(C/T) &= (C/T)_{\text{Ce}} - (C/T)_{\text{La}} \\ &= \gamma_{\text{Ce}} + \beta T^2 - (\gamma_{\text{La}} + \beta T^2) = \gamma_{\text{Ce}} - \gamma_{\text{La}} \quad (2) \end{aligned}$$

gives the value of the electronic specific-heat coefficient for the cerium-containing compound in excess of the electronic contribution to heat capacity of the corresponding lanthanum compound, and one would expect that this difference will be temperature independent when the influence of the anomaly-causing phenomena becomes negligible. After averaging these temperature-independent differences and adding γ_{La} , obtained from a least-squares fit of the experimental data to Eq. (1), we have determined the γ 's for the cerium compounds (Table II). The temperature regions in which parameters were determined are also indicated. The electronic specific-heat constant values for these three compounds

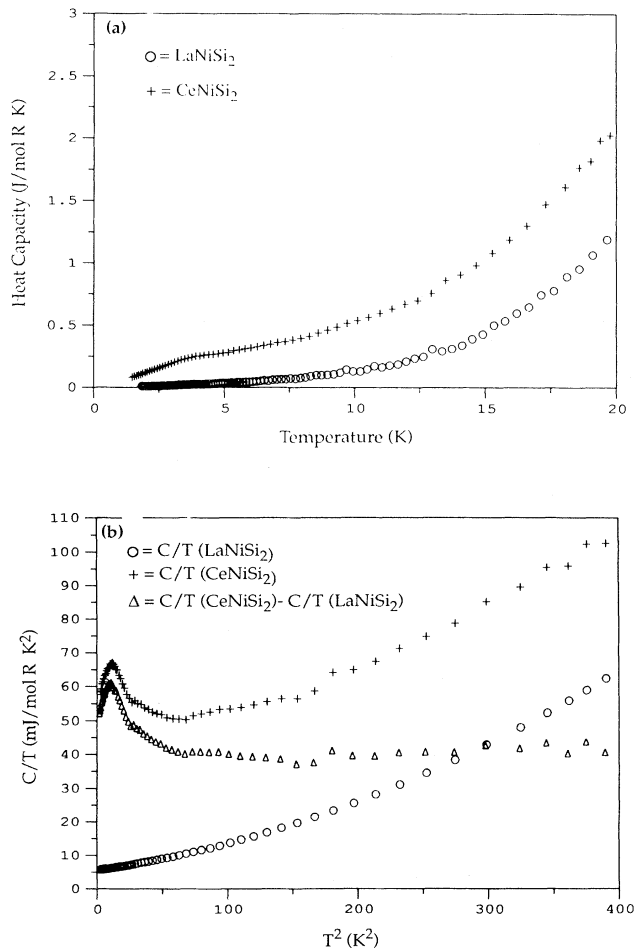


FIG. 1. (a) Zero-field heat-capacity data for LaNiSi_2 and CeNiSi_2 ; (b) the C/T vs T^2 plots and the difference $\Delta(C/T) = C/T(\text{CeNiSi}_2) - C/T(\text{LaNiSi}_2)$.

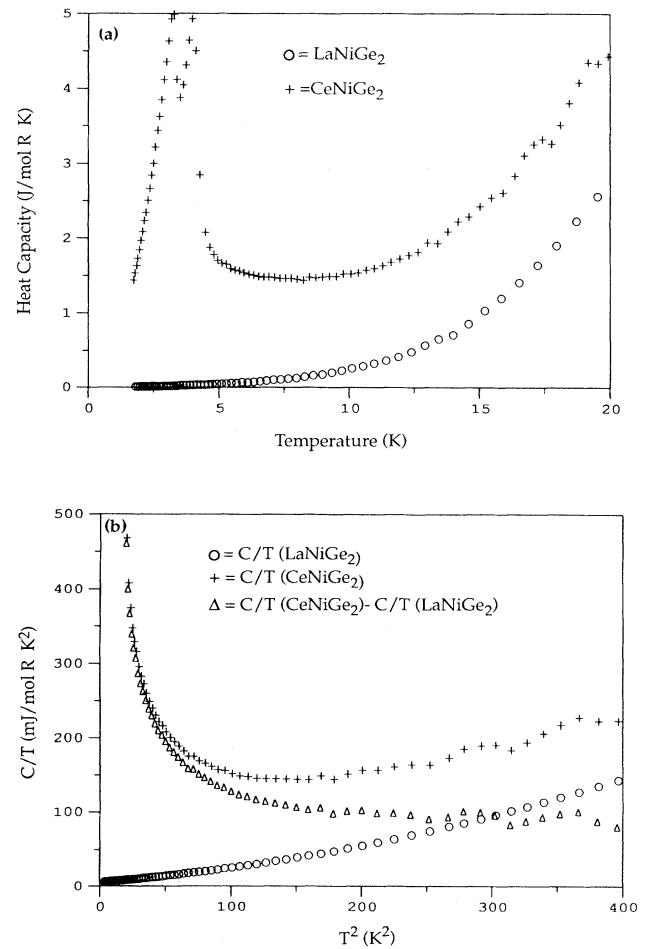


FIG. 2. (a) Zero-field heat-capacity data for LaNiGe_2 and CeNiGe_2 ; (b) the C/T vs T^2 plots and the difference $\Delta(C/T) = C/T(\text{CeNiGe}_2) - C/T(\text{LaNiGe}_2)$.

TABLE II. Electronic specific-heat coefficients and Debye temperatures^a of investigated compounds.

Compound	γ (mJ/mol R K ²)	Θ_D (K)	Temperature range	
			Fitting (K)	Const. diff. (K)
LaNiSi ₂	5.26(7) ^b	451(2) ^b	< 12	
CeNiSi ₂	45.3(6)	451		> 9
LaNiGe ₂	5.60(1)	351(1)	< 10	
CeNiGe ₂	97.6(9)	351		> 14
LaNiSn ₂	5.6(1)	258(2)	< 5	
CeNiSn ₂	60.8(7)	258		> 14

^aDebye temperatures for Ce-containing compounds are assumed to be the same as in the corresponding La phase.

^bA least-squares estimated standard deviation in the least significant digit is given in parentheses.

are rather typical for cerium intermetallic compounds, although the value for CeNiGe₂ suggests that it may be considered a heavy fermion.

The heat capacity of CeNiSe₂ [Fig. 1(a)] shows an al-

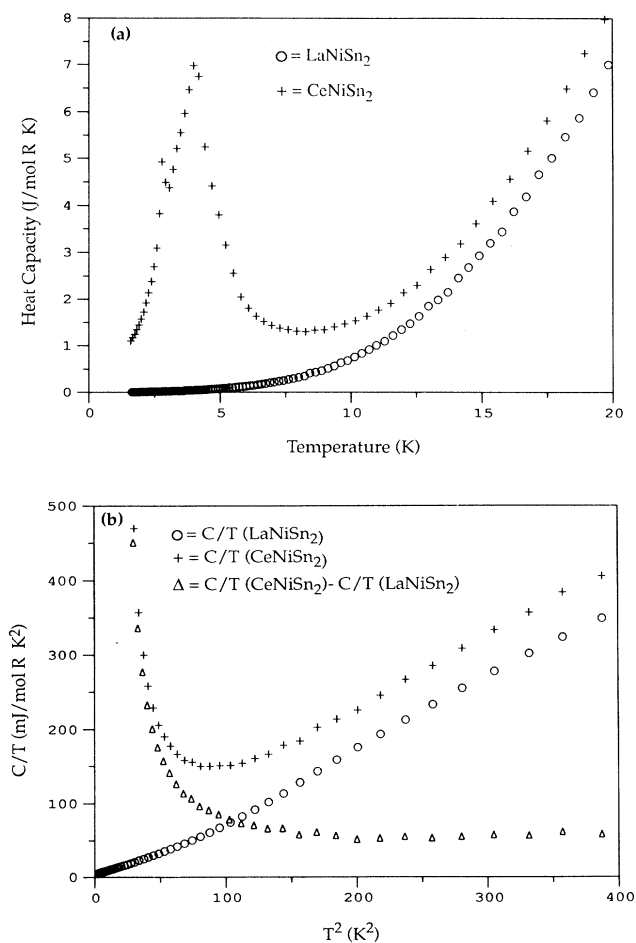


FIG. 3. (a) Zero-field heat-capacity data for LaNiSn₂ and CeNiSn₂; (b) the C/T vs T^2 plots and the difference $\Delta(C/T) = C/T(\text{CeNiSn}_2) - C/T(\text{LaNiSn}_2)$.

most linear (and a high rate) increase with temperature from 1.5 to ~ 3.5 K, and then more slowly until at about 9 K it starts to behave like the LaNiSi₂ heat capacity, but still it has a much larger magnitude than that of LaNiSi₂. The first noted feature can be seen much clearer from the C/T versus T^2 plot [Fig. 1(b)], which is characterized by the presence of a small bump at 3.3 K.

The heat capacities of LaNiGe₂ and CeNiGe₂ are presented in Fig. 2(a). The two sharp maxima of approximately equal magnitude (~ 5.0 J/mol K) at 3.2 and 3.9 K in CeNiGe₂ are obvious. Above ~ 14 K the influence of the phenomena which caused these maxima becomes negligible, and the heat capacity of CeNiGe₂ [Figs. 2(a) and 2(b)] has a temperature dependence which parallels that of LaNiGe₂.

Figure 3(a) is a plot of C versus T , and Fig. 3(b) a plot of C/T versus T^2 for LaNiSn₂ and CeNiSn₂. The heat capacity of CeNiSn₂ is similar to that of CeNiGe₂ in that there are two maxima below 5 K. The lowest one is characterized by a peak value of ~ 5 J/mol K, which is the same as that in the germanium compound, but it occurs at a somewhat lower temperature (2.6 K). However, as discussed in the next section, we believe that because of overlap in the heat capacity from the high-temperature ordering transition, the apparent ordering temperature of the low-temperature magnetic transition as deduced from the heat-capacity data appears to be 2.6 K, but that the true ordering temperature for the lower transition is 3.2 K. The upper peak has a significantly higher magnitude (~ 7 J/mol K), but occurs at exactly the same temperature as observed for the CeNiGe₂ phase (3.9 K). As in the previous case, above ~ 14 K the heat capacities of LaNiSn₂ and CeNiSn₂ have parallel slopes.

It is not difficult to see that we have found two different types of heat-capacity anomalies: the first is observed for CeNiSi₂ and is characterized by a low magnetic entropy (64.6 mJ/mol(Ce) K) and thus is not likely to be due to any type of magnetic ordering which involves the complete lattice of $4f^1$ electrons. Nor is it due to any impurities, since metallography revealed that this sample was completely free of any observable second phase. The second is found in CeNiGe₂ and CeNiSn₂, and is characterized by the presence of two sharp λ -type maxima which are typical for magnetically ordered systems and

have large entropies associated with them: 3.05 (52.9%) and 4.21 J/mol(Ce) K (73.1% of the theoretically expected value $R \ln 2$), respectively.

Magnetic susceptibilities

The inverse magnetic susceptibility of CeNiSi_2 is illustrated in Fig. 4(a) for the whole temperature region, and in Fig. 4(b) the low-temperature details are enlarged. Contrary to that reported in Ref. 3, it obviously does not obey the Curie-Weiss law up to 300 K and is characterized by the weak temperature dependence and the presence of a broad minimum at ~ 100 K. Below 50 K, the magnetic behavior is distinctly different. The high-temperature (50–300 K) region behavior is typical for compounds with fluctuating valences (between Ce^{3+} and Ce^{4+}). A simple model, which describes the features for a fluctuating valence in a cerium material, was developed by Sales and Wohleben.⁷ The temperature dependence of the magnetic susceptibility was given as

$$\chi = N(2.54\mu_B)^2\nu(T)/3k_B(T + T_{sf}), \quad (3)$$

where $T + T_{sf}$ is the replacement of the thermodynamic temperature by an effective one, and $\nu(T)$ is the temperature- and energy-dependent function of fractional occupation Ce^{3+} and Ce^{4+} states and is given by

$$\nu(T) = 6 / \{6 + \exp[E_{ex}/k_B(T + T_{sf})]\} \quad (4)$$

with E_{ex} being the energy difference between the two states Ce^{3+} and Ce^{4+} .

The solid line drawn through the experimental data in Figs. 4(a) and 4(b) represents the results of a successful fit using Eqs. (3) and (4), with an extra difference—the addition of the temperature-independent value of χ_0 . We believe χ_0 is composed of the temperature-independent Van Vleck, conduction-electron paramagnetic, and the core-electrons diamagnetic contributions. The values of the parameters obtained by fitting the experimental data are quite reasonable: $T_{sf} = 183.6(9)$ K, $-E_{ex}/k_B = 549(1)$ K, and $\chi_0 = 1.65(1) \times 10^{-6}$ emu/g (the last number is about 25% of the average mass susceptibility in this temperature range). At low temperature, the susceptibility [see Fig. 4(b)] changes slope at the same point (~ 3.3 K) as a bump found to be present on heat-capacity data (Fig. 1).

Figure 5 shows the theoretical estimate of the temperature dependence of the cerium valence as derived from Eq. (4) using the previously determined least-squares-fit parameters T_{sf} and E_{ex} . As one can see, in the temperature region where $\chi(T)$ obeys the Sales and Wohleben model⁷ (50–300 K), the cerium valence effectively increase in magnitude from mostly Ce^{3+} ions at room temperature (a mean value of +3.35) to mostly Ce^{4+} ions at 50 K (a mean value of +3.65).

The magnetization at 2, 3, and 4 K was linear with field from 100 to 1000 Oe and the intercept passed through the origin. This indicates that the small peak in

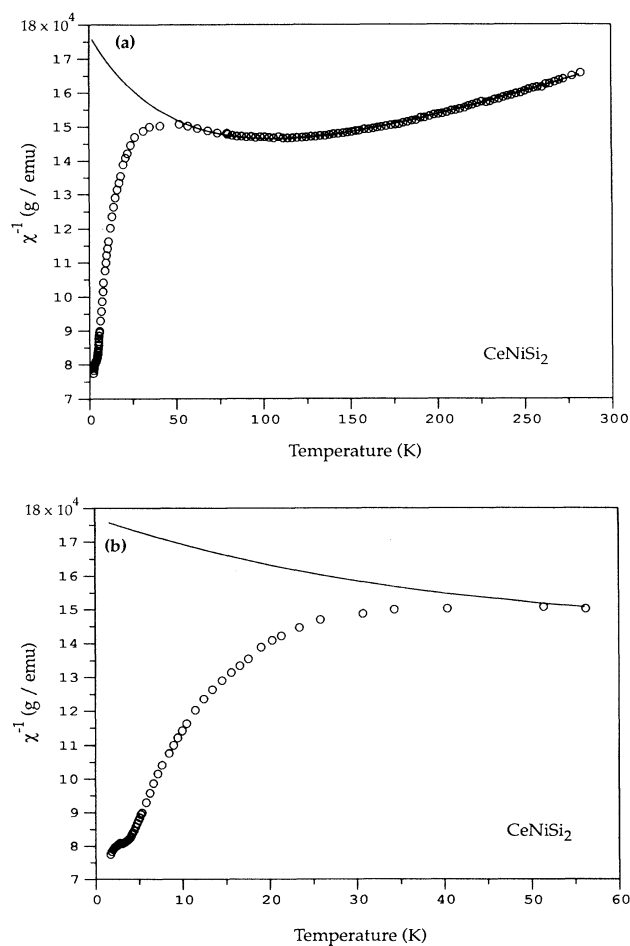


FIG. 4. (a) Inverse magnetic susceptibility of the CeNiSi_2 ; (b) the low-temperature region in detail. The solid line drawn through the experimental data represents a successful fit of the experimental data to the model of Sales and Wohleben (Ref. 7).

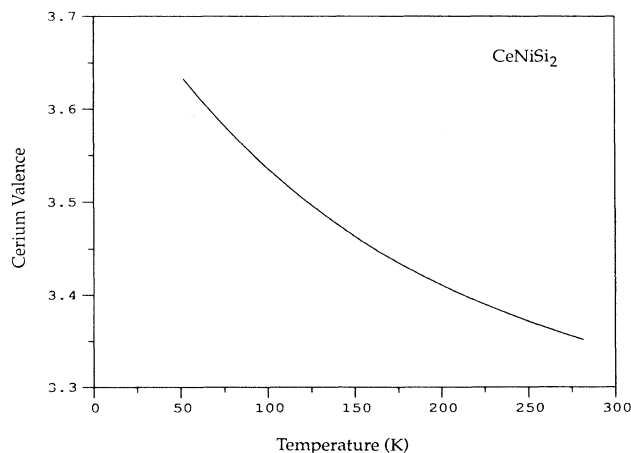


FIG. 5. The effective valence of the cerium in CeNiSi_2 as a function of temperature.

the heat capacity at zero field is not due to magnetic ordering.

Although the inverse magnetic susceptibility (Fig. 4) shows a sharp drop (by about a factor of 2), the actual

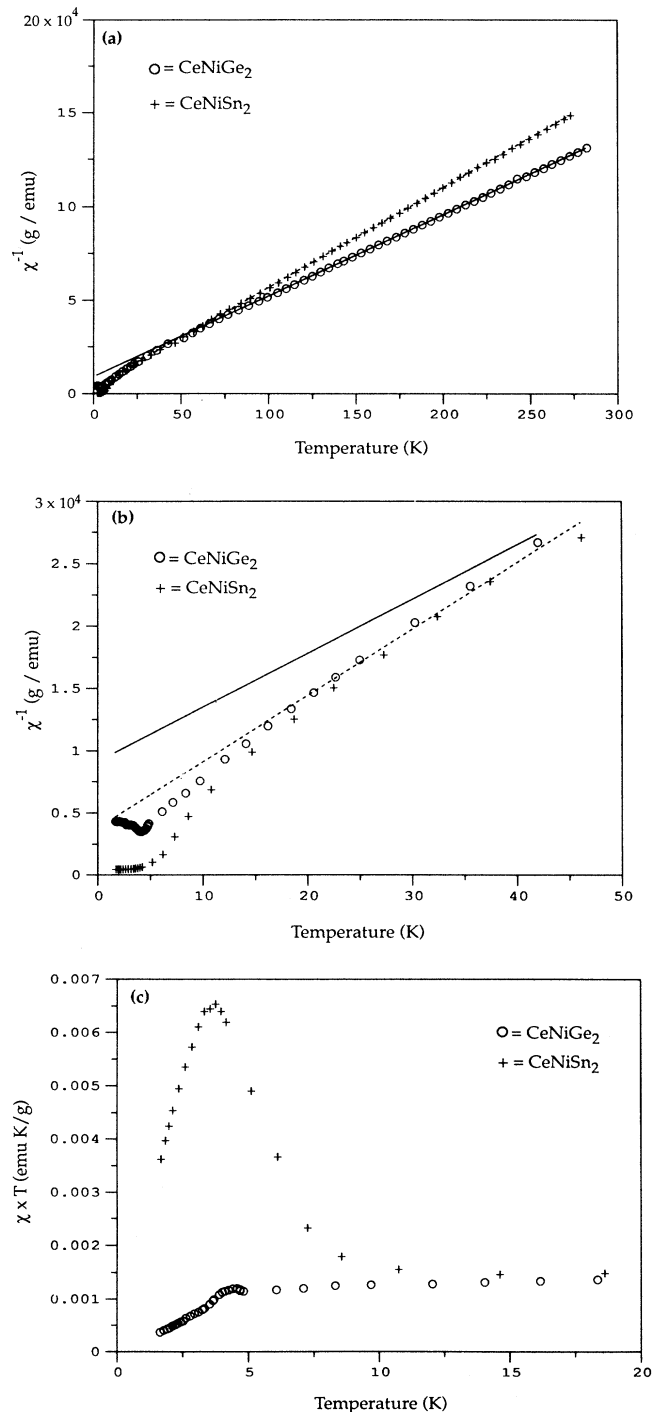


FIG. 6. (a) Inverse magnetic susceptibilities of the compounds CeNiGe₂ and CeNiSn₂; (b) the low-temperature details as χ^{-1} vs T and (c) as χT vs T plots. Lines drawn through the experimental data represent Curie-Weiss behavior.

magnetic susceptibility is quite small at ~ 2 K ($\sim 3200 \times 10^{-6}$ emu/mol Ce), more than 1 order of magnitude smaller than that of CeNiGe₂ and nearly 2 orders of magnitude smaller than that of CeNiSn₂ [see Figs. 6(a) and 6(b)]. This strongly suggests that Ce is not in or even approaching an ordered magnetic state as the temperature goes to zero. The magnitude is consistent with a mixed valence state with a valence of 3.5 or greater. This point is further discussed in the next section, which deals with the the magnetic heat capacity of CeNiSi₂.

The inverse magnetic susceptibilities of CeNiGe₂ and CeNiSn₂ are shown in Figs. 6(a)–6(c). Both compounds obey Curie-Weiss above $T=50$ K, which allows us to determine effective paramagnetic moments and the paramagnetic Curie temperatures. They are: $\mu_{\text{eff}}=2.52(1)\mu_B$ and $\theta_p=-20.8(5)$ K for CeNiGe₂ and $\mu_{\text{eff}}=2.56(1)\mu_B$ and $\theta_p=-6.9(3)$ K for CeNiSn₂. The characteristic values for the last compound are close to those reported earlier by Skolozdra and Komarovskaya.² In both cases, effective magnetic moments agree quite well with the theoretical value expected for the free Ce³⁺ ion ($2.54\mu_B$), which implies that the magnetism in these compounds is due to the cerium-ion sublattice only, and the nickel is nonmagnetic.

Consistent with the heat-capacity data (see Figs. 2 and 3) and the small and negative paramagnetic Curie temperatures, both compounds undergo antiferromagnetic phase transitions at lowest temperatures. Figure 6(b) shows these low temperatures χ^{-1} versus T curves in more detail. In the case of CeNiGe₂ it is clear even from this curve that the magnetic order has an antiferromagnetic nature, but for CeNiSn₂ it is not so obvious. For CeNiSn₂ one can see only a change of slope rather than the beginning of an upturn at ~ 4 K. The type of ordering becomes much clearer in a plot of χT versus T for CeNiSn₂ [Fig. 6(c)]. The obvious decrease of χT below ~ 4 K is a good confirmation of an antiferromagnetically ordered ground state of the compound with tin.

The magnetic susceptibility and heat-capacity data for CeNiGe₂ and CeNiSn₂ show that neither system undergoes a simple one-step antiferromagnetic ordering phase transition, but that the nature of the antiferromagnetism is more complicated. Both measurements show that (1) the high-temperature antiferromagnetic phase (we will call it phase II) is quite visible and exists over a small temperature interval (3.2–3.9 K); and (2) below 3.2 K both compounds with germanium and tin change their magnetic structures into a more stable phase, which is labeled phase I. Earlier we noted that the lower-temperature heat-capacity maximum in CeNiSn₂ is located at 2.6 K, but the susceptibility data show that the slope changes for both phases occur practically at the same temperatures [Fig. 6(c)]. We believe that the observed lower heat-capacity maximum at 2.6 K in the case of CeNiSn₂ is simply caused by overlapping with the upper transition, which has a greater magnitude and thus the true temperature is that observed in the magnetic susceptibility data. Therefore, the Néel temperatures for both CeNiGe₂ and CeNiSn₂ are $T_N^{\text{II}}=3.9$ K, and $T_N^{\text{I}}=3.2$ K, and in each of these systems two different types of an-

tiferromagnetic structures occur even with only one independent magnetic (Ce) atom per unit cell.

Small cubic-shaped pieces were cut from the arc-melted rodlike ingot and annealed samples of CeNiGe_2 and LaNiGe_2 for low-field, low-temperature magnetization measurements. X-ray diffractometry revealed the presence of a preferred grain orientation in both samples, which was not too surprising. This preferred orientation is consistent with the unit-cell dimensions (a and c are of about the same length, and b is much longer) in that such a unit cell usually caused the existence of platelike crystallites which easily form a preferably oriented, as-cast sample. Even though both samples were not well grain-aligned, it was sufficient to find out that both CeNiGe_2 and LaNiGe_2 are magnetically anisotropic with an easy axis parallel to the $[010]$ crystallographic direction. The magnetic susceptibility of LaNiGe_2 is temperature independent, and its magnitude shows that it is an extremely weak paramagnet, displaying neither thermal nor magnetic hysteresis, with average susceptibility about 10^3 times lower than that for CeNiGe_2 . These data are consistent with the above conclusion about the absence of magnetic moments localized on the nickel-atom sublattice.

The two-step antiferromagnetic phase transition occurring in the CeNiGe_2 is much clearer from low-field ($H=1000$ G) susceptibility measurements (Fig. 7). Unfortunately, the grain alignment was not perfect, and the difference between both curves is small. Nevertheless, one can see that when the field was directed parallel to the longest crystallographic axis (b), the susceptibility anomalies are sharper than in the case of the perpendicular field orientation. This peculiarity might be evidence that the antiferromagnetic I-II transition occurs with spins aligned in different ways along or at least close to the b axis. While measuring the magnetization as a func-

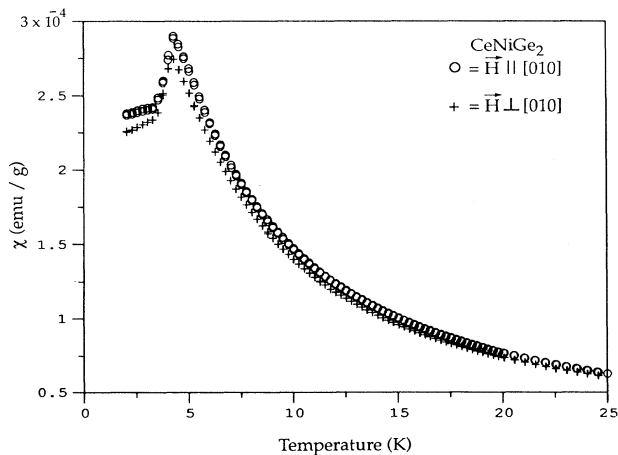


FIG. 7. Low-field ($H=1000$ G) low-temperature susceptibility data measured from a sample of the compound CeNiGe_2 with preferred orientation along and perpendicular to the $[010]$ crystallographic direction.

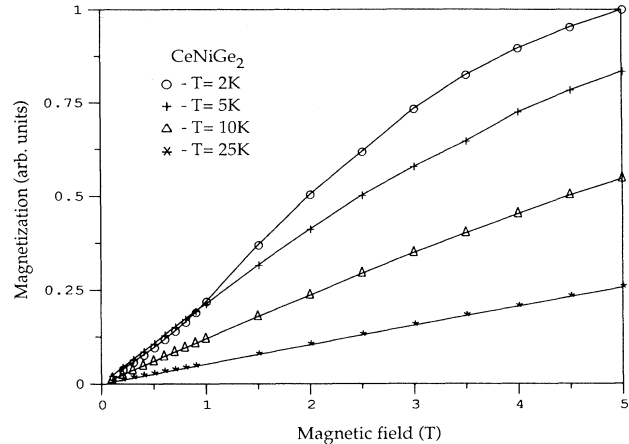


FIG. 8. The magnetization isotherms of the CeNiGe_2 . Solid lines drawn through the data points are guides for the eye.

tion of the external magnetic field, we also found that a metamagnetic spin-flip phase transition occurs in CeNiGe_2 at $T=2$ K when the applied field exceeded about 1 T (Fig. 8).

Magnetic heat capacity of CeNiSi_2

The zero-field heat-capacity and magnetic-susceptibility data described above shows that the compound containing silicon (CeNiSi_2) exhibits quite unusual magnetic behavior: (1) at high temperatures (50–300 K) it is obviously a typical valence fluctuating system with an effective cerium valence varying from +3.35 (~ 300 K) to +3.65 (50 K); and (2) because of such a partially delocalized nature of the cerium $4f$ electrons, a spin-fluctuating behavior at low temperatures is quite possible.

As already mentioned above, one can see a small bump in the zero-field C/T versus T^2 curve [Fig. 1(b)] appearing at the same temperature where a slope anomaly is observed in the susceptibility data [see Fig. 4(b)]. It is known that a sufficiently high magnetic field can quench spin fluctuations and accordingly suppress the spin-fluctuation contribution to the electronic heat capacity. Thus the total heat capacity should be decreased by the field (see, for an example, papers by Ikeda and Gschneidner⁸ and Gschneidner and Dhar⁹). Figures 9(a) and 9(b) show the high magnetic-field heat capacity of CeNiSi_2 together with zero-field data. The bump still exists at $H=2.46$ T, and it is nearly suppressed at $H=5.32$ T and completely so by a 9.85 T magnetic field, consistent with theoretical predictions for spin fluctuators. Another important observation is that an obvious upturn at temperatures just below the bottom of the bump is induced even by the lowest applied field of 2.46 T. This upturn is slightly shifted toward higher temperatures as the magnetic field is increased. Right above the bump ($T > \sim 4.5$ K) the magnetic field causes a gentle enhancement of the CeNiSi_2 total heat capacity.

We have also considered that the heat-capacity bump

at ~ 3 K might be due to spin-glass behavior, but since fields > 5 T are required to quench this peak, we can rule out spin-glass behavior, since fields of only 1 T are sufficient to destroy spin-glass behavior in lanthanide spin-glass materials. This is also consistent with low-field (100–1000 Oe) magnetization, which showed that no magnetic ordering is occurring 2, 3, or 4 K.

All of these peculiarities may be understood from the point of view that CeNiSi₂ around $T=3.3$ K (the temperature where both magnetic susceptibility and zero-field heat-capacity anomalies are present) is about ready to undergo an antiferromagnetic phase transition, but the nearly delocalized nature of the cerium 4*f* electrons make the magnetic interactions so weak that the system is in a state of confusion. This competition causes both the increasing of the entropy associated with the bump on the C/T versus T^2 curve and the slope anomaly for the susceptibility data, but finally the system remains weakly paramagnetic. The relatively low applied magnetic field ($H < 2.5$ T) cannot suppress this spin-fluctuation state at

temperature around 3.3 K, but at $T < 2$ K it helps to align the weak cerium magnetic moments causing the weak ferromagnetic behavior of CeNiSi₂, which is seen as a low-temperature upturn and a high-temperature enhancement of $C/T(T)$.

CONCLUSION

The six compounds $RNiX_2$ ($R=La, Ce$ and $X=Si, Ge,$ and Sn) represent a series with substitution either of the rare-earth metal with an empty 4*f* level (lanthanum) by cerium, which has a single 4*f* electron, or the semiconducting silicon by metallic tin or the intermediate germanium. All intermetallides have the same crystal structure—the orthorhombic CeNiSi₂ type. Both kinds of substitutions have a significant influence on physical behaviors: (1) in all cases, the substitution of lanthanum by cerium causes a remarkable increase in the density of states at the Fermi level and therefore in the electronic contribution to the heat capacity (γ rises from more than eight times for $RNiSi_2$ to more than 17 times for $RNiGe_2$). (2) For lanthanum-containing compounds, γ remains independent by interchanging from Si to Ge to Sn, while the Debye temperature decreases dramatically (see Table II), much more than might be expected from mass change on going from Si to Ge to Sn, i.e., $\Theta_D \propto M^{-1/2}$, where M is the molecular mass of the compound. One can estimate the Debye temperatures of LaNiGe₂ and LaNiSn₂ to be 376 and 333 K, respectively, relative to that of LaNiSi₂ from just the mass change on substituting Ge and Sn for Si. As one notes, these calculated values are significantly higher than the measured values of 351 and 258 K, respectively. The additional reduction in Θ_D is consistent with the lattice “softening” caused by a weakening of the interatomic interactions due to both a change in the chemical nature of these three elements from mostly covalent to more metallic properties, and to the increase of the average interatomic distances in the above series of compounds. (3) The enhancement of the electronic specific-heat coefficient (γ) does not completely correlate with Si-Ge-Sn substitution in the cerium-containing compounds. There is an increase in γ on substituting either Ge or Sn for Si ($\gamma=45.3$ mJ/molCe K² for CeNiSi₂) but the highest value was found for CeNiGe₂ ($\gamma=97.6$) rather than for the Sn compound ($\gamma=60.8$). The high γ value for CeNiGe₂ places it in the low-effective-mass heavy-fermion class of materials.

Consistent with closer chemical behaviors of germanium and tin than between germanium and silicon, the CeNiGe₂ and CeNiSn₂ compounds are much more similar to one another than with CeNiSi₂, even in their magnetic behaviors. For example, the antiferromagnetic ordering temperatures ($T_N^I=3.2$ K) and ($T_N^{II}=3.9$ K) are the same for both phases. On this basis we believe that they will have closely related magnetic structures.

The unusual magnetic and valence behaviors of the cerium in CeNiSi₂ are quite unexpected, although there is some evidence for a cerium valence state slightly greater than 3 when one considers the lattice constants (especially *b*) and the unit-cell volume of the CeNiSi₂ relative to

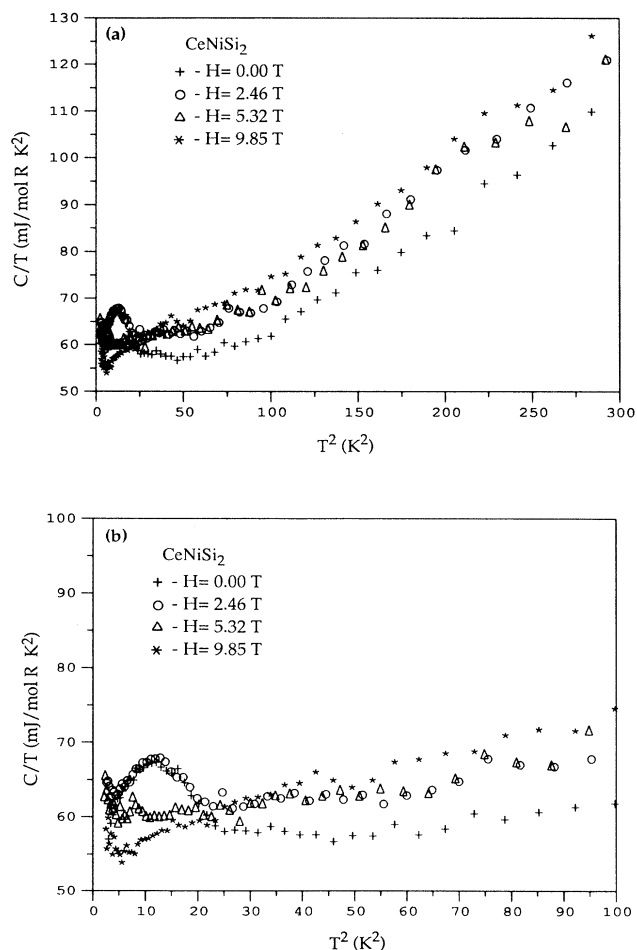


FIG. 9. The high-magnetic-field heat capacity of the compound CeNiSi₂ as C/T vs T^2 plots: (a) over the temperature region $1.4 \text{ K} < T < 17 \text{ K}$ ($2 \text{ K}^2 < T^2 < 300 \text{ K}^2$); (b) the low-temperature details at $1.4 \text{ K} < T < 10 \text{ K}$ ($2 \text{ K}^2 < T^2 < 100 \text{ K}^2$).

cerium's nearest neighbors in the periodic system (the same compounds with La, Pr, and Nd) at room temperature. The presence of a slight room-temperature minimum of the unit-cell volume (i.e., a valence of ~ 3.1) is somewhat consistent with the estimated effective cerium valence (3.35) as determined from the magnetic-susceptibility data. At 300 K it is near Ce^{3+} rather than in the Ce^{4+} state, and as the temperature is lowered the valence increases ($v_{\text{eff}} = +3.65$ at $T = 50$ K), and we think that at low temperature, the unit-cell-volume anomaly at cerium would become more evident.

Note added in proof. Recently Geibel *et al.*¹⁰ noted that CeNiSi_2 is a mixed valence compound, and that CeNiGe_2 orders antiferromagnetically at 4 K. No other details were reported. These results are in good agree-

ment with the data presented in our study, except that we found two antiferromagnetic ordering temperatures in CeNiGe_2 .

ACKNOWLEDGMENTS

The Ames Laboratory is supported by the Office of Basic Energy Science, U.S. Department of Energy by Iowa State University under Contract No. W-7405-ENG-82. The financial support of V.K.P. by the International Research & Exchange Board (IREX) is also acknowledged. The authors would like to thank Dr. J. Tang and J. O. Moorman for help with some low-temperature heat-capacity and magnetic-susceptibility measurements.

*Permanent address: Department of Inorganic Chemistry, L'vov State University, L'vov, 290005, U.S.S.R.

¹O. I. Bodak and E. I. Gladyshevsky, *Kristallografiya*, **14**, 990 (1969) [*Sov. Phys.-Crystallogr.* **14**, 859 (1970)].

²R. V. Skolozdra and L. Komarovskaya, *Izv. Akad. Nauk SSSR Met.* [2], 214 (1988) [*Russ. Metall. Met.* [2], 207 (1988)].

³O. I. Bodak, E. I. Gladyshevsky, E. M. Levin, and R. V. Lutsiv, *Dopov. Akad. Nauk Ukr. RSR Ser. A*, 1129 (1977).

⁴K. Ikeda, K. A. Gschneidner, Jr., B. J. Beaudry, and U. Atzmony, *Phys. Rev. B* **25**, 4604 (1982).

⁵R. J. Stiermann, K. A. Gschneidner, Jr., T. -W. E. Tsang, F. A. Schmidt, P. Klavins, R. N. Shelton, J. Queen, and S. Legvold, *J. Magn. Mater.* **32**, 4519 (1985).

⁶L. G. Akselrud, Yu. N. Gryn', P. Yu. Zavalij, V. K. Pecharsky, and V. S. Fundamensky (unpublished).

⁷B. C. Sales and D. K. Wohlleben, *Phys. Rev. Lett.* **35**, 1240 (1975).

⁸K. Ikeda and K. A. Gschneidner, Jr., *Phys. Rev. Lett.* **45**, 1341 (1980).

⁹K. A. Gschneidner, Jr. and S. K. Dhar, in *Magnetic Excitation and Fluctuations*, edited by S. W. Lovesey, U. Balucani, F. Borsa, and V. Tognetti (Springer-Verlag, Berlin, 1984), p. 177.

¹⁰C. Geibel, C. Kämmerer, E. Göring, R. Moog, G. Sparr, R. Henseleit, G. Cordier, S. Horn and F. Steglich, *J. Magn. Mater.* **90-91**, 435 (1990).